In Silico Pharmacology (2022) 10:14
https://doi.org/10.1007/s40203-022-00130-4

ORIGINAL RESEARCH

Docking simulation and ADMET prediction based investigation on the phytochemical constituents of Noni (*Morinda citrifolia*) fruit as a potential anticancer drug

Kaliraj Chandran[1] · Drose Ignatious Shane[1] · Azar Zochedh[1] · Asath Bahadur Sultan[2] · Thandavarayan Kathiresan[1]

Received: 19 April 2022 / Accepted: 5 August 2022

Abstract
Morinda citrifolia is a traditional plant used in Asian and African countries for its wide nutraceutical and therapeutic effects for the treatment of various ailments. The fruit of *M. citrifolia* has various biological properties such as anti-bacterial, anti-oxidant, anti-cancer. Using the molecular docking based investigation; we explored around twenty three bioactive phytochemicals in *M. citrifolia* fruit against human cancer. MAPK6 (mitogen-activated protein kinase 6) was selected as target protein and these twenty three phytochemicals along with a known MAPK6 inhibitor were docked against the target protein. The docking scores of the bioactive phytochemicals against MAPK6 protein range between − 4.5 kcal/mol to − 7.9 kcal/mol and the docking score of the standard drug (CID: 447077) was − 7.3 kcal/mol. Based on the binding affinity five phytochemicals asperuloside (− 6.7 kcal/mol), asperulosidic acid (− 7.2 kcal/mol), deacetylasperulosidic acid (− 7.0 kcal/mol), eugenol (− 6.8 kcal/mol) and rutin (− 7.9 kcal/mol) were chosen for further evaluation. These five compounds were further investigated through RC plot analysis, density function theory and ADMET properties. Stable linkage of protein–ligand interaction was observed through RC plot, density function theory showed the structural stability and reactivity of bioactive compounds through the energy gap between HOMO and LUMO and the ADMET (adsorption, distribution, metabolism, excretion and toxicity) studies showed the safety profile of the bioactive compounds. These in silico results support the utilization of *M. citrifolia* fruit in the traditional medication and the initiation for the development of new drug against human cancer through in vivo and in vitro evaluation.

Keywords *Morinda citrifolia* · MAPK6 · Molecular docking · DFT · ADMET

Introduction

Cancer is characterized as an unregulated cell or tissue development that might spread to different parts of the body. It is the second most prominent reason for mortality in the world, behind cardiovascular illnesses and the number of cases keeps on rising day by day (Mallath et al. 2014). Globally, 19.30 million new cancer cases and 10 million cancer deaths were reported by GLOBOCON 2020 (Erratum: Global Cancer Statistics 2018, 2020). A range of modifiable wellbeing ways of behaving for example, simple carbohydrate diet and high fat, irregular dietary patterns as well as poor physical work adds to the unexpected ascent in cancer incidences (Kushi et al. 2010). Previous reports have shown that the sedentary lifestyle and dysregulated nutrition are major contributors to the redox process in cells, resulting in unintended by-products such as reactive oxygen species (ROS), DNA reactive aldehyde and reactive nitrogen species (RNS) (Perše 2014; Ren et al. 2018; Viswanathan et al. 2022). ROS is an inevitable byproduct of mitochondrial oxidative phosphorylation (Palmeira et al. 2019) that has both beneficial and detrimental effects. ROS regulates cell cycle, differentiation, proliferation and migration at low concentration and damage nucleic acids, lipids, proteins, membranes and organelles at higher concentration and also diminishes cell viability and cause apoptosis (Nordberg and Arnér 2001; Ganesan et al. 2018). Antioxidant prevention mechanisms

✉ Azar Zochedh

Thandavarayan Kathiresan
t.kathiresan@klu.ac.in

[1] Department of Biotechnology, Kalasalingam Academy of Research and Education, Krishnankoil, Tamilnadu, India

[2] Department of Physics, Kalasalingam Academy of Research and Education, Krishnankoil, Tamilnadu, India

Published online: 25 August 2022

neutralize production of reactive oxygen species (ROS). Cells and tissues were protected from oxidative stress and toxins by detoxifying and antioxidant enzymes (Sachdev et al. 2021) and ROS scavenging was accomplished by oxidative stress sensitive genes by secreting antioxidant enzymes (Mates 2000). Down regulation of cellular antioxidant pathways and enzyme systems was caused due to the increases level of intracellular ROS that leads to malignant transformation through different molecular targets like nuclear factor erythroid-2-related factor 2 (Nrf2), nuclear factor-B (NF-B), phosphoinositide 3-kinase (PI3K), Kelch-like ECH-associated protein 1 (Keap1) and mitogen-activated protein kinases (MAPKs) (Xiao et al. 2013). MAPKs are a class of threonine or serine protein kinases that execute significant role in controlling extracellular signaling into a broad range of cellular processes (Roux and Blenis 2004). Depending upon their functions and structure, they are divided into atypical and conventional MAPKs. Atypical MAPKs like extracellular signal–regulated kinase (ERK) 3/4 and ERK 7/8 and conventional MAPKs are p38 isoforms (α, β, γ, and δ) and ERK 1/2 (Cargnello and Roux 2011). The ERK 1/2 AND p38 MAPK pathways have been designated by various medications to fight the different types of malignant growth with some clinical achievement. When compared to conventional ERK 1/2 MAPKs, considerably less work has been investigated on ERK3, otherwise called MAPK6 signaling (Alsaran 2016). The ERK3 play a vital physiological function together with pulmonary differentiation, angiogenesis and T cell activation. Moreover, MAPK6 has been interfacing a series of signaling cascades and assume a significant role in the progression and invasiveness of certain kinds of carcinomas. Both in normal and tumorigenic cells, MAPK6 is essential for the creation of many cellular factors including interleukin-8 (IL-8) (Bogucka et al. 2020). MAPK6 is generally expressed protein in all tissues with highest expression levels detected in brain, skeletal muscle and gastrointestinal tract (Long et al. 2012).

Therapeutic plants produce different sorts of bioactive compounds, making them sources of various kinds of possible medications (Walton and Brown 1999; Ghasemzadeh et al. 2010). Indeed, therapeutic plants are a significant legacy for mankind and specifically, for most of poor communities in developing nations who rely upon them for their essential medical needs and livelihoods (Salhi et al. 2010). This isn't simply because of the low economic resources of the populaces in these nations that limit the purchase of drugs, yet in addition the ineffectiveness of a few synthetic drugs (Conlon et al. 2003). Therefore, various plants are great sources of therapeutic agents and are customarily utilized for various purposes, including medicines against virus, bacteria and fungi (Bessong et al. 2006). *Morinda citrifolia* is one of the therapeutic plants with wide nutraceutical properties and known for its therapeutic qualities beginning around 2000 years in Asia and Australia (Whistler 1985). It is type of subtropical and tropical plant widely seen on the Pacific islands and has been utilized to treat around 2000 diseases (McClatchey 2002). It is also utilized as anti-bacterial, anti-inflammatory, anti-fungal, analgesic, anti-parasitic and anti-cancer (Calzuola et al. 2006; Wang et al. 2002; Jasril et al. 2003; Pawlus et al. 2005; Potterat and Hamburger 2007; Ruksilp et al. 2011). In USA the fruit juice of *M. citrifolia* is marketed as a dietary supplement under the name "Noni" (Phakhodee 2012). In Benin this plant was recently introduced for the treatment of urinary tract infection, cough, tuberculosis, skin infection, etc. Fresh or Fermented natural pure juice from fruit without addition of water are often used. There is very little evidence supporting the medicinal values of *M. citrifolia* fruit. Thus, this study was focused to do the phytochemicals screening and to evaluate the anti-cancer activity of *M. citrifolia* fruit using molecular docking approach against appropriate cancer receptor protein MAPK6 and drug-likeness evaluation based on ADMET (absorption, distribution, metabolism, excretion, and toxicity) properties of selected bioactive phytochemicals.

Methodology

Protein retrieval and preparation

The X-ray crystallographic structure of MAPK6 protein (PDB ID: 7AQB) was retrieved from RCSB Protein Data Bank (PDB: http://www.rcsb.org/pdb) (Berman et al. 2000). Prior to docking, the protein was prepared by adding the missed residues using Swiss-PDB viewer v4.1.0. Then by using BIOVIA Discovery studio v4.0 software (Accelrys Software Inc., San Diego, CA, USA) to remove existing ligands and water molecules and was saved in ".pdb" format, that was used for molecular docking analysis.

Active compounds retrieval

We found that around 23 bioactive phytochemicals were found in *M. citrifolia* fruit from Dr. Duke's Phytochemical and Ethnobotanical database (https://phytochem.nal.usda.gov). The 3D structures of these twenty three bioactive compounds and a known MAPK6 inhibitor (CID: 447077) were retrieved from PubChem database (https://pubchem.ncbi.nlm.nih.gov/) (Mohanraj et al. 2018).

Active site identification

Active site or binding site in the target protein is a particular site on a protein that allows the ligand to attach and execute a reaction. The active site of the target protein MAPK6 (PDB

ID: 7AQB) was identified and validated using CASTp (Computed Atlas of Surface Topography of proteins) online web tool (http://sts.bioe.uic.edu/castp/index.html?3trg). This program aids us in comprehending all active sections as well as necessary information for the target protein. It utilizes PDB or Job ID in the case of uploading the prepared target structure. On the processing, numerous pockets get appear and the ideal pocket was determined using the total area and the volume of active regions present within target structure.

Molecular docking

Molecular docking is a widely used computational technique in the process of drug design. PyRx 0.8 free available software was used to accomplish the docking analysis (Dallakyan et al. 2015). The bioactive phytochemicals were the ligand molecules and the protein of target was MAPK6 (PDB ID: 7AQB). Initially, selected five ligand molecules along with the standard drug (CID: 447077) were imported in the graphical window. Then all the ligands were minimized and converted to ".pdbqt" format. The target protein was then loaded and made as macromolecules and converted into ".pdbqt" format. The grid box was built at the binding pockets and the docking was performed. Finally, the results were analyzed and saved in ".csv" format. From the PyRx results, the best five compounds (asperuloside, asperulosidic acid, deacetylasperulosidic acid, eugenol and rutin) with high docking scores were selected. The output files of docked ligand molecules and the target protein were loaded on BIOVIA Discovery studio v4.0 tool. The type of bond interactions, number of hydrogen bonds and bond distances were analyzed. The complex and interaction images of protein with ligand both in 2D and 3D were also obtained using Discovery studio. Then the Ramachandran plot (RC plot) was built through the chart option in discovery studio and the position of interacted amino residues in the RC plot was evaluated.

ADMET evaluation

The physiochemical, absorption, distribution, metabolism, excretion, and toxicity model analysis of selected bioactive compounds with the top binding scores based on molecular docking results were evaluated using pkCSM (http://biosig.unimelb.edu.au/pkcsm/prediction) online tool. The canonical SMILES used for study of these compounds were retrieved from PubChem online database (https://pubchem.ncbi.nlm.nih.gov) (Wang et al. 2019).

Density function theory

In a pharmacological activity of a drug-like molecule electronic effect plays a vital role. Density function theory (DFT) is a significant theory for analyzing the electronic states of solids, molecules and atoms through three-dimensional electronic density system (Novena et al. 2022). DFT helps for quantitative understanding of molecules through fundamental laws of quantum chemicals. In this present study, the selected phytochemicals with top binding scores through molecular docking were performed using Gaussian 09 W Program. The DFT/B3LYP technique with the 6–311++ G(d,p) basis set was used to optimize the molecular structure of the selected bioactive compounds. Frontier molecular orbitals (FMO) energies LUMO (lowest unoccupied molecular orbital), HOMO (highest occupied molecular orbital) and their energy gap (LUMO–HOMO) was calculated for the selected bioactive compounds.

Results

Active site prediction

Active site regions of the target protein MAPK6 was analyzed through CASTp online tool. From the CASTp results the most ideal active site region with their active pockets were analyzed. Even though the active site regions of the MAPK6 was known, the CASTp helps to cover more potential pockets in the active regions of the target protein MAPK6 through their ideal scores. The results of CASTp shows the number of ideal pockets and the chains present in the active regions of the target protein. In the target protein MAPK6, the residues present in chain A was analyzed to be in the active regions. The total of 17 pockets were predicted using CASTp, out of which an ideal pocket containing the area of 18,318.8 SA was selected as an active region (Fig. 1a) which has the following residues of A_108, A_109, A_110, A_111, A_112, A_113, A_114, A_156, A_159, A_169, A_170, A_171, A_172, A_26, A_31, A_34, A_35, A_47, A_49, A_65, A_69, A_78, A_80. The Fig. 1b denotes the various sequences which contribute to the formation of active site in those specific regions. These residues were chosen and used for selective docking based on which the interaction profile can be analyzed. These active site regions of the target protein MAPK6 was utilized during the process of molecular docking. By utilizing these active site regions the grid box was made in the target protein for the ligand to be docked. By docking at active regions the binding affinity may be stronger and docking scores will be better for ligands.

Molecular docking analysis

The molecular docking was performed to analyze the binding capability of twenty three bioactive phytochemicals against the target protein MAPK6. In this study, a standard

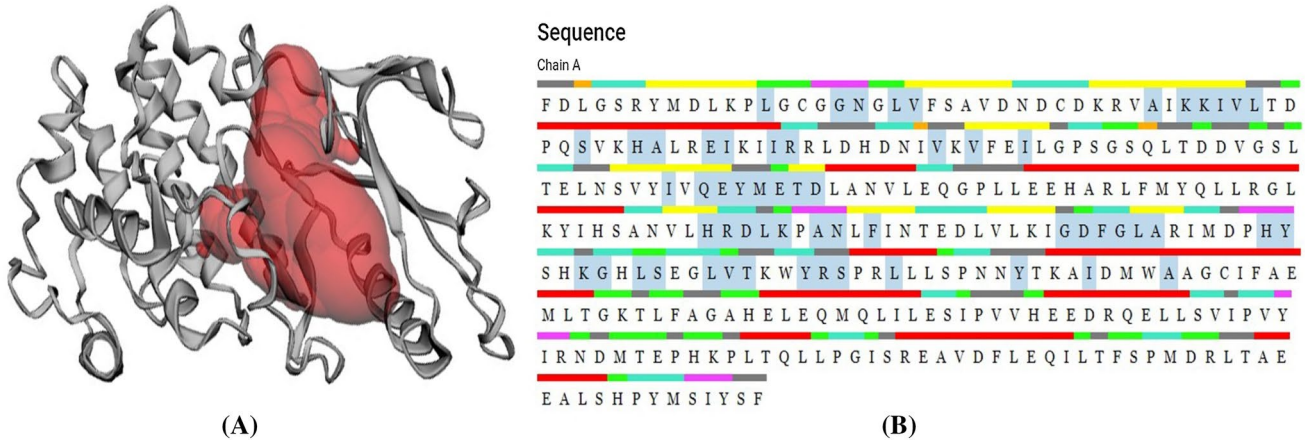

Fig. 1 Predicted active site region of target protein MAPK6. **A** Active site region of MAPK6. **B** Sequence involved in formation of active site in MAPK6

MAPK6 inhibitor (CID: 447077) was utilized as a control, due to the previously reported inhibitory potential against Bcr-Abl-dependent cell growth in various cell lines with IC50 values ranges from 2 to 35 nM (Wisniewski et al. 2002). The binding affinity of the bioactive phytochemicals was found to be scattered from range of −4.5 to −7.9 kcal/mol and the binding scores of the twenty three bioactive phytochemicals along with the standard MAPK6 inhibitor was shown in Table 1. Five bioactive compounds were shown to have high binding energy (> −6.5 kcal/mol) with the target protein MAPK6. The top five bioactive compounds Asperuloside (−6.7 kcal/mol), Asperulosidic acid (−7.2 kcal/mol), Deacetylasperulosidic acid (−7.0 kcal/mol), Eugenol (−6.8 kcal/mol) and Rutin (−7.9 kcal/mol) were selected for future evaluation based on their binding affinity at the active site of target protein MAPK6. The lowest binding affinity was found with the phytochemical Caproic acid with the binding score of −4.5 kcal/mol. Also, the docking score of known MAPK6 inhibitor was −7.3 kcal/mol, whereas the bioactive compound rutin showed better binding affinity when compared to the standard and Asperulosidic acid (−7.2 kcal/mol), Deacetylasperulosidic acid (−7.0 kcal/mol) has shown good binding affinity similar to known MAPK6 inhibitor. These lead bioactive compounds, which has strong bonding and good docking scores as compared to reference drug. Therefore these lead molecules could be used as an antagonist of the target protein MAPK6 to prevent cancer. These docking scores of the bioactive phytochemicals with the target protein showed binding potential of phytochemicals against targeted cancer protein MAPK6 (Table 2).

Table 1 Binding affinity of bioactive phytochemicals of *Morinda citrifolia* fruit with MAPK6

S. no.	PubChem CID	Phytochemicals	Binding affinity (Kcal/mol)
1	84298	Asperuloside	−6.7
2	11968867	Asperulosidic acid	−7.2
3	243	Benzoic acid	−5.8
4	244	Benzyl alcohol	−5.7
5	5280489	Beta carotene	−6.3
6	8892	Caproic acid	−4.5
7	379	Caprylic acid	−5.0
8	12315350	Deacetylasperulosidic acid	−7.0
9	2969	Decanoic acid	−5.1
10	637517	Elaidic acid	−5.0
11	12366	Ethyl Palmitate	−4.8
12	3314	Eugenol	−6.8
13	5793	Glucose	−5.2
14	8892	Hexanoic acid	−4.7
15	3893	Lauric acid	−5.1
16	22311	Limonene	−6.5
17	5280450	Linoleic acid	−5.2
18	11005	Myristic acid	−4.7
19	17249752	Nananoic acid	−5.0
20	379	Octanoic acid	−5.2
21	985	Palmitic acid	−4.8
22	5280805	Rutin	−7.9
23	5280460	Scopoletin	−6.5
24	447077	Known MAPK6 inhibitor	−7.3

It was observed that compound asperuloside (CID: 84298) formed one (1) donor conventional hydrogen bond interaction with MET111 at bond distance 2.40305 Å and two (2) acceptor carbon hydrogen bond interactions with amino residues GLU112 and ASP114 with 3.02657 Å and 3.5938 Å bond distances. Asperulosidic acid (CID: 11968867) with target protein MAPK6 formed one (1) donor and three (3) acceptor conventional hydrogen bond

Table 2 List of amino acid residues and bond category between selected five bioactive compounds against MAPK6

Compounds (CID)	Residues	Amino acid	Bond category
Asperuloside (CID: 84298)	111	MET	Hydrogen bond
	112	GLU	Hydrogen bond
	114	ASP	Hydrogen bond
Asperulosidic acid (CID: 11968867)	108	GLN	Hydrogen bond
	112	GLU	Hydrogen bond
	114	ASP	Hydrogen bond
	114	ASP	Hydrogen bond
	113	THR	Hydrogen bond
Deacetylasperulosidic acid (CID: 12315350)	111	MET	Hydrogen bond
	111	MET	Hydrogen bond
	109	GLU	Hydrogen bond
	171	ASP	Hydrogen bond
	156	ALA	Hydrogen bond
Eugenol (CID: 3314)	108	GLN	Hydrogen bond
	171	ASP	Hydrogen bond
	159	PHE	Hydrophobic
	26	LEU	Hydrophobic
	47	ALA	Hydrophobic
	34	VAL	Hydrophobic
	34	VAL	Hydrophobic
	110	TYR	Hydrophobic
	159	PHE	Hydrophobic
	47	ALA	Hydrophobic
	78	VAL	Hydrophobic
Rutin (CID: 5280805)	31	ASN	Hydrogen bond
	31	ASN	Hydrogen bond
	49	LYS	Hydrogen bond
	50	LYS	Hydrogen bond
	171	ASP	Electrostatic
	61	HIS	Hydrophobic
	34	VAL	Hydrophobic
	34	VAL	Hydrophobic

interactions with GLU108, GLU112, ASP114 (2) at 2.00682 Å, 2.88175 Å, 2.57924 Å and 2.38571 Å bond distances and one (1) carbon hydrogen bond interaction with THR113 at 3.59702 Å. Target protein MAPK6 with our compound deacetylasperulosidic acid (CID: 12315350) formed two (2) donor conventional hydrogen bond interactions with MET111 (2) at 2.34431 Å and 2.25824 Å distances and three (3) acceptor hydrogen bond interactions with amino acid residues GLU109, ASP171 and ALA156 at bond distances 2.07156, 2.47858 and 2.60879 Å, respectively. Our compound Eugenol (CID: 3314) with MAPK6 formed one (1) donor conventional hydrogen bond interaction with GLN108 at 2.87334 Å and one (1) acceptor carbon hydrogen bond interaction with ASP171 at 3.75442 Å distance. Also Eugenol with MAPK6 formed one (1) Pi-stacked, four (4) Alkyl and four (4) Pi-alkyl hydrophobic bond interactions with PHE159, LEU26, ALA47, VAL34 (2), TYR110, PHE159, ALA47 and VAL 78 at 3.91126, 3.73834, 3.73348, 5.46227, 3.98096 Å, 4.7341, 5.04285, 4.45872 and 5.35103 Å bond distances. For Rutin (CID: 5280805) it has been observed three (3) donor conventional hydrogen bond interactions with ASN31 (2) and LYS49 and one (1) acceptor conventional hydrogen bond interaction with LYS50 at bond distances 2.12557, 2.43091, 2.2582 and 2.76755 Å and three (3) Pi-Alkyl hydrophobic bond interactions with HIS61 and VAL34 (2) at 5.20239, 5.06848 Å and 4.36038 Å distances. Other interaction includes one Pi-Anion electrostatic interaction with amino residue ASP171 at bond distance 4.10825 Å (Figs. 2, 3, 4, 5, 6).

Ramachandran plot (RC plot) analysis

The Ramachandran plot, often known as the RC plot, is used to depict the secondary structures of proteins using the

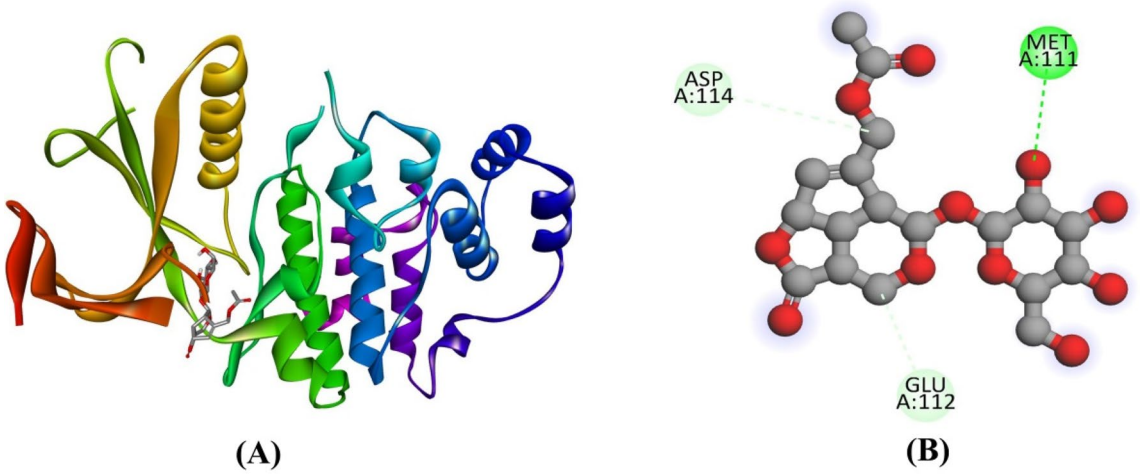

Fig. 2 Interaction of bioactive compound Asperuloside with MAPK6. **A** Complex structure. **B** 2D interaction

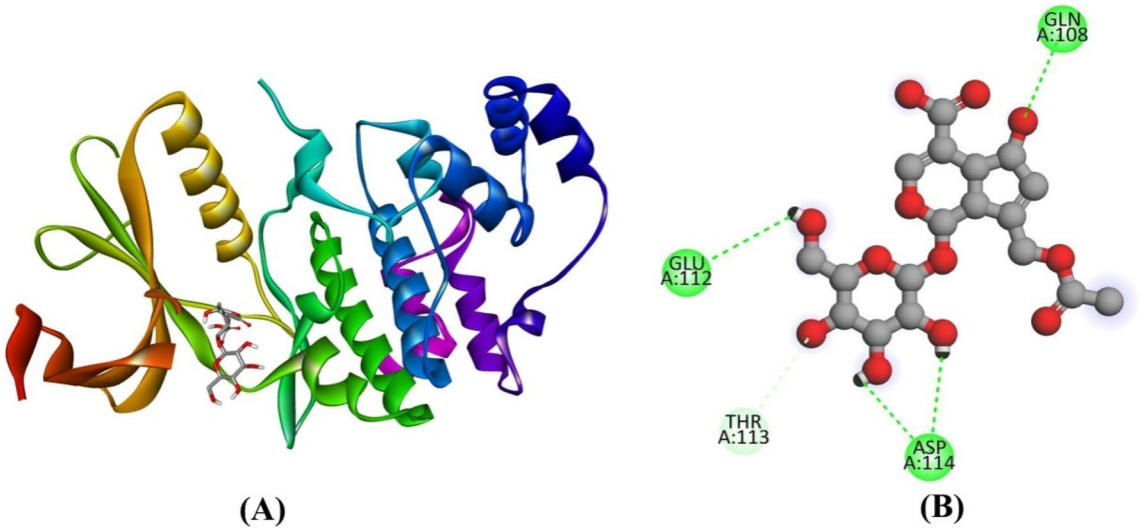

Fig. 3 Interaction of bioactive compound Asperulosidic acid with MAPK6. **A** Complex structure. **B** 2D interaction

amino acid dihedral angles φ and ψ. This assists in determining the amino acid rotations that may occur within that protein. We can also evaluate the overall stability of the bonded protein–ligand complex based on their ideal location within the plot. According to the RC plot interpretation against the protein–ligand complex, the plain white region denotes the unfavorable rotations of the φ and ψ bonds in the specific complex. The purple zone on the surface indicates less favorable rotation limits, whereas the blue area denotes more favorable rotation limits. The MAPK6-Asperuloside complex possesses a bond rotation in a highly favorable zone, according to the visualization in Fig. 7A. It is also expected to contain a β-sheet as its bonded secondary structure, which will be combined with the right-handed α helix. In comparing the MAPK6-Asperulosidic Acid complex in Fig. 7B, β-sheets were found in abundance in the highly favorable zone, followed by a single right-handed α-helix in conjunction as their secondary structure. On examining the MAPK6-Deacetylasperulosidic acid complex shown in Fig. 7C, a mixture of β-sheets with left and right-handed α helix was discovered. Figure 7D, E show that β sheets and few α-helix in the highly favorable zone have identical bond rotations, indicating that the protein–ligand complex interaction has a stable linkage based on the secondary structure and its rotation prospective. Table S1 represents the percentage of alpha-helix and beta-sheet in the protein–ligand interactions of the lead compounds. From table S1 it was analyzed that in asperuloside and MAPK6 interaction the percentage of right-handed alpha helix was 50% and the beta-sheet was 50%, in asperulosidic acid and MAPK6

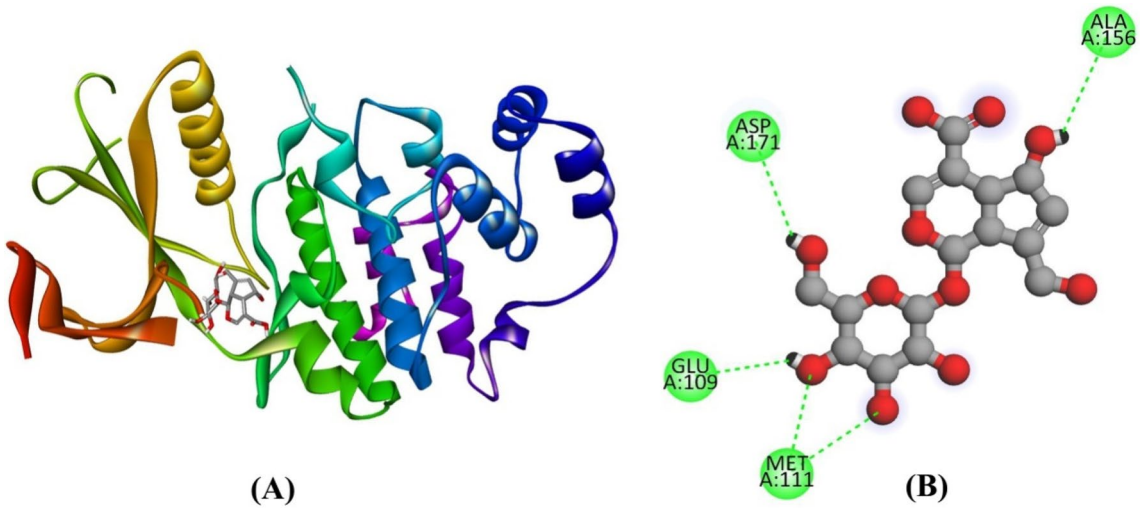

Fig. 4 Interaction of bioactive compound Deacetylasperulosidic acid with MAPK6. **A** Complex structure. **B** 2D interaction

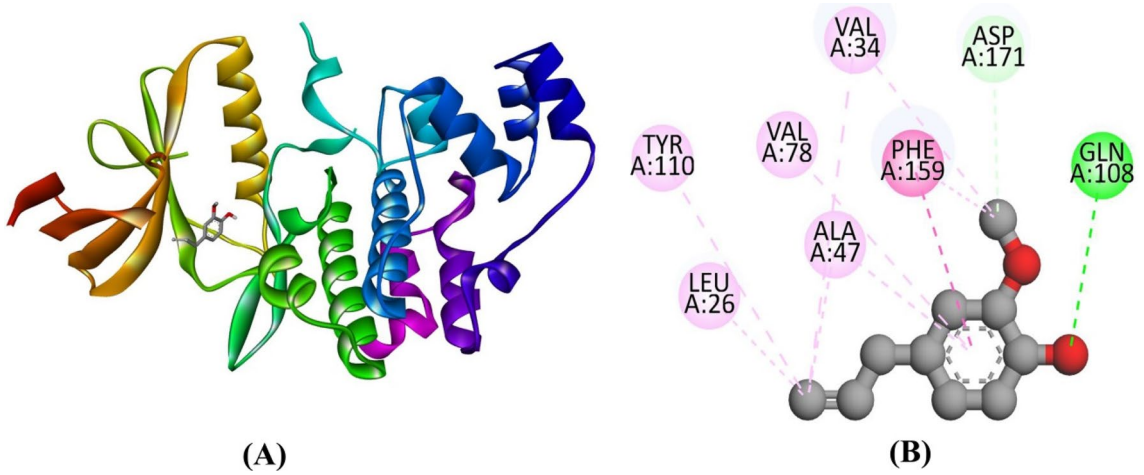

Fig. 5 Interaction of bioactive compound Eugenol with MAPK6. **A** Complex structure. **B** 2D interaction

interaction the percentage of right-handed alpha-helix was 12.5% and beta-sheet was 87.5%, in deacetylasperulosidic acid with MAPK6 interaction the percentage of right-handed alpha-helix was 25%, left-handed alpha-helix was 25% and beta-sheet was 50%, in compound eugenol and MAPK6 interaction the percentage of right-handed alpha-helix was 12.5%, left-handed alpha helix was 12.5% and beta-sheet was 75% and in rutin and MAPK6 interaction the percentage of right-handed alpha-helix was 28.6%, left-handed alpha-helix was 14.3% and beta-sheet was 57.1% respectively.

Density function theory

The calculation of frontier molecular orbitals (FMOs) determines by what means a molecule interacts with the other species. The frontier molecular orbitals are the lowest unoccupied molecular orbital (LUMO) and the highest occupied molecular orbital (HOMO). The FMO measurements deal records on the energy gap between LUMO and the HOMO states. The LUMO is an electrophile that receives electrons from the nucleophile, while the HOMO is a nucleophile, which provides electrons (Prashanth et al. 2016; Zhuo et al. 2012). FMO can furthermore be used to determine the stability of a molecule. A molecule with a lower energy gap is understood to be softer because it is extremely polarizable and has good chemical reactivity, whereas a molecule with a greater energy gap is said to have worthy stability and high chemical hardness (Al-Omary et al. 2015; Zochedh et al. 2022). The selected top binding bioactive compound's LUMO and HOMO energies, energy gap, and related molecular factors were calculated by using B3LYP method with a 6–311++G(d,p) basis set. The

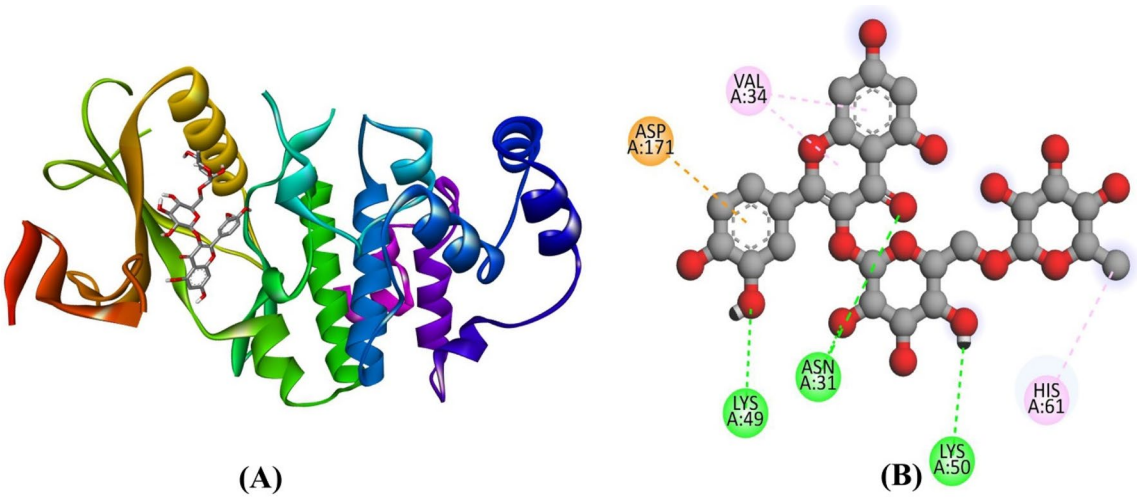

Fig. 6 Interaction of bioactive compound Rutin with MAPK6. **A** Complex structure. **B** 2D interaction

global reactivity descriptors, electron affinity (A), ionization potential (I), chemical potential (μ), electronegativity (χ), softness (S), global hardness (η) and electrophilicity index (ω) may be estimated using Koopmans' theorem and the energies of HOMO and LUMO of the selected top binding bioactive compounds. Figure S1 to figure S5 depict the FMOs plot of the selected top five bioactive compounds. The calculated energy gap ($\Delta E = E_{LUMO} - E_{HOMO}$) between LUMO and HOMO of the selected bioactive molecules has been calculated to be 5.816968 eV (Asperuloside), 5.31247 eV (Asperulosidic acid), 5.71274 eV (Deacetylasperulosidic acid), 5.41533 eV (Eugenol) and 4.79192 eV (Rutin) respectively. Table 3 represents all of the results. According to the Koopmans' theorem, negative energies of HOMO and LUMO are ionization potential (I) and electron affinity (A). I = − EHOMO; A = − ELUMO; Electronegativity (χ) is defined by $\chi = (I + A)/2$; chemical potential (μ) is a negative of electronegativity $\mu = -(I + A)/2$; chemical hardness (η) is defined by $\eta = (I - A)/2$; chemical softness (S) was inverse of chemical hardness $S = 1/\eta$; electrophilicity index of, $\omega = \mu^2/2\eta$; nucleophilicity (N) was inverse of electrophilicity, $N = 1/\omega$. The chemical potential and electronegativity are estimated from the values of I and A. Among the five selected bioactive compounds, rutin showed less energy gap that shows chemical reactivity of will be higher when compared to other bioactive compounds, whereas the asperuloside showed highest energy value that exhibits that it possesses better strength and stability than other compounds. The great stream of electrons in the middle of donor (HOMO) and the acceptor (LUMO) brings about lowering of energy considered to be electrophilicity index (Zochedh et al. 2022) and the compound eugenol showed lowest electrophilicity index of, ω = 1.553336 eV and nucleophilicity index (N) was higher with the eugenol and lower with the asperuloside.

ADME evaluation of selected bioactive compounds

The physiochemical properties or drug-likeness properties of the selected bioactive phytochemicals were analyzed through online tool pkCSM. The physiochemical properties were evaluated during the drug discovery to analyze whether the lead molecule satisfies the Lipinski's rule of five. Lipinski's rule of five was an important factor during the development of oral drug discovery. The lead molecules satisfying the Lipinski's rule of five with violation or with maximum of one violation can only be considered as oral drug. The data in Table 4 revealed the result of physiochemical properties of selected phytochemicals. The drug-likeness evaluation was done based on Lipinski's Rule of Five. The Lipinski's rule states that molecular weight should be less than 500; hydrogen bond donor and Log P value should not exceed 5, hydrogen bond acceptor and rotatable bonds should be 10 or less than 10. No more than one rule can be violated. Rutin was found to have the highest molecular weight of 610.521 g/mol, followed by asperuloside acid with 432.378 g/mol, asperuloside with 414.363 g/mol, deacetylasperulosidic acid with 390.341 g/mol and eugenol with 164.204 g/mol. Likewise, the surface area and lipophilicity of the phytochemicals: Asperuloside, asperulosidic acid, deacetylasperulosidic acid, eugenol and rutin are 164.608, 170.089, 152.878, 72.109 and 240.901 $Å^2$ and − 2.296, − 2.7759, − 3.3467, 2.1293 and − 1.6871 respectively. The compound eugenol does not violate any Lipinski's rule. The Lipinski's rule of five was evaluated only for the oral drugs; hence the cancer is treated by intravenous medication, the violation of Lipinski's rule cannot be a big issue

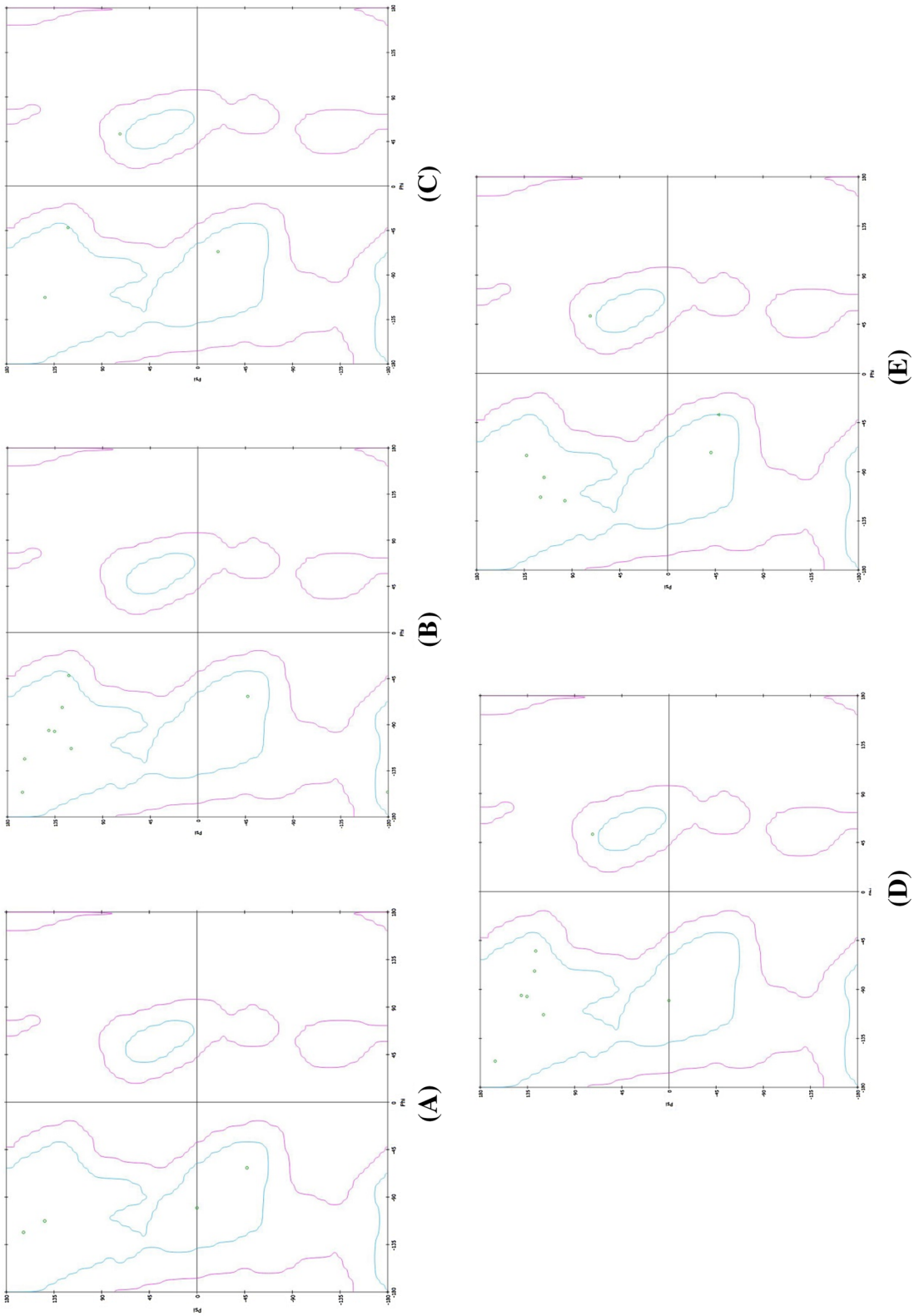

Fig. 7 Ramachandran plot of interacted amino residues with the lead compounds. **A** Asperuloside, **B** Asperulosidic acid, **C** Deacetylasperulosidic acid, **D** Eugenol and **E** Rutin

Table 3 Calculated FMOs and related molecular properties values of selected bioactive phytochemicals using B3LYP/6−311++G (d, p) basis set

Parameters (eV)	Asperuloside	Asperulosidic acid	Deacetylasperulosidic acid	Eugenol	Rutin
E_{LUMO}	−0.98804	−1.06069	−0.60055	−0.19265	−0.94423
E_{HOMO}	−6.805008	−6.37316	−6.31329	−5.60798	−5.73615
$\Delta(E_{LUMO} - E_{HOMO})$	5.816968	5.31247	5.71274	5.41533	4.79192
Electron affinity (A)	0.98804	1.06069	0.60055	0.19265	0.94423
Ionization potential (I)	6.805008	6.37316	6.31329	5.60798	5.73615
Chemical hardness (η)	2.9084	2.656235	2.85637	2.707665	2.39596
Chemical potential (μ)	−3.896524	−3.716925	−3.45692	−2.900315	−3.34019
Electronegativity (χ)	3.896524	3.716925	3.45692	2.900315	3.34019
Electrophilicity Index (ω)	2.610181	2.600585	2.091868	1.553336	2.328267
Nucleophilicity (N)	0.3831152	0.384529	0.4780416	0.6437757	0.429504
Chemical softness (S)	0.343832	0.3764727	0.350095	0.369322	0.417369

Table 4 ADME evaluation of selected bioactive phytochemicals

Descriptor	Asperuloside	Asperulosidic acid	Deacetylasperulosidic acid	Eugenol	Rutin
Molecular weight (g/mol)	414.363	432.378	390.341	164.204	610.521
Lipophilicity (log P)	−2.296	−2.7759	−3.3467	2.1293	−1.6871
No. of rotatable bonds	5	6	5	3	6
No. of acceptors	11	11	10	2	16
No. of donors	4	6	7	1	10
Surface area ($Å^2$)	164.608	170.089	152.878	72.109	240.901
Water solubility (log mol/L)	−3.276	−2.529	−2.767	−2.25	−2.892
Caco2 permeability (log Papp)	0.383	−0.41	−0.54	1.559	−0.949
Human intestinal absorption (%)	51.524	14.878	0.139	92.041	23.446
Skin permeability (log Kp)	−2.795	−2.735	−2.735	−2.207	−2.735
P-glycoprotein substrate	Yes	Yes	Yes	No	Yes
P-glycoprotein I inhibitor	No	No	No	No	No
P-glycoprotein II inhibitor	No	No	No	No	No
VDss (human) (log L/kg)	−0.019	−0.26	−0.976	0.24	1.663
Fraction unbound (human) (Fu)	0.589	0.608	0.673	0.251	0.187
BBB permeability (log BB)	−1.439	−1.58	−1.193	0.374	−1.899
CNS permeability (log PS)	−3.789	−3.902	−3.913	−2.007	−5.178
CYP2D6 substrate	No	No	No	No	No
CYP3A4 substrate	No	No	No	No	No
CYP1A2 inhibitor	No	No	No	Yes	No
CYP2C19 inhibitor	No	No	No	No	No
CYP2C9 inhibitor	No	No	No	No	No
CYP2D6 inhibitor	No	No	No	No	No
CYP3A4 inhibitor	No	No	No	No	No
Total clearance (log ml/min/kg)	1.219	1.307	1.351	0.282	−0.369
Renal OCT2 substrate	No	No	No	No	No

for cancer drugs. Our compound eugenol showed highest water solubility of −2.25 and asperuloside showed the least water solubility of −3.276. Also eugenol has the highest Caco2 (Human colon adenocarcinoma-2) permeability of 1.559 and can easily absorbed by the Human intestinal cells with 92.041% whereas; rutin has the lowest permeability range of −0.949. All the phytochemicals except eugenol are substrate of P-glycoprotein. None of the selected bioactive

compounds are the inhibitor of P-glycoprotein I and P-glycoprotein II. The steady state volume distribution (VDss) was relatively low for all the phytochemicals except rutin. Rutin showed VDss value of 1.663. The results also revealed that deacetylasperulosidic acid showed highest unbound fraction of human blood. Eugenol readily crosses Blood–Brain Barrier (BBB) and Central Nervous System (CNS) whereas; other phytochemicals have very poorly BBB permeability and unable to penetrate CNS. All the selected compounds were not CYP2D6 and CYP3A4 substrate. Also, all the phytochemicals were not CYP1A2, CYP2C9, CYP2C19, CYP2D6 and CYP3A4 inhibitor, except eugenol which showed inhibition of CYP1A2. Deacetylasperulosidic acid has the highest and rutin has the lowest total clearance value of 1.351 and − 0.369. None of the selected phytochemicals is the renal organic transporter (OCT2) substrate.

Predicted toxicity values of selected phytochemicals

The toxicological profiles of all selected phytochemicals were resulted in Table 5. All the phytochemicals has no AMES toxicity (mutagenic potential against bacteria) except eugenol. All the phytochemicals are not the inhibitors of hERG I and hERG II except rutin. Rutin showed inhibitory property of hERG II. Low values of maximum tolerated dosage were showed in all the phytochemicals. The LD50 values of phytochemicals: Asperuloside, asperulosidic acid, deacetylasperulosidic acid, eugenol and rutin are 2.262, 2.344, 2.154, 2.118 and 2.491 mol/kg and the LOAEL values are 3.426, 3.641, 3.362, 2.049 and 3.673 log m/kg respectively. The predicted values showed that all the phytochemicals has no hepatotoxicity and except eugenol all phytochemicals showed no skin sensitization.

Discussion

The major reason for this research is to identify and analyze the various properties of the bioactive compounds present in *M. citrifolia* fruit using phytochemical screening followed by molecular docking and ADMET analysis. Phytochemical screening is a systematic process that outlines the key to identifying the various phytochemicals present in the fruit we've chosen for the study. *M. citrifolia* fruit was rich in butyric acid smell and flavor and it is consumed in the majority of countries (Chan-Blanco et al. 2006). It is identified in this case to evaluate the MAPK6 inhibition mechanism. We were able to narrow down the work of researchers in the area of identifying the role of the Noni plant in cancer suppression owing to this study. We can predict several different approaches for this specific pharmaceutical medication by analyzing the binding affinity and its interaction profile. In molecular docking, hydrogen bond interaction, bond category, distance of the bond between the amino residue and the docked compounds and docking scores of the bioactive compounds against the targeted protein MAPK6 at their active site regions play a vital role in the effective binding of bioactive compounds and target protein. The selected bioactive compounds showed hydrogen bond interactions and other bond interactions with amino residues present at the active regions of target protein (Ahmed et al. 2014). Based on the Ramachandran plot analysis of interacted protein and ligand showed that selected bioactive compounds were in the highly favorable zone with identical bond rotations, representing that the protein–ligand complex interaction has a stable linkage based on structure and its rotation prospective. The band gap energy ΔE of the selected bioactive compounds ranges between 4.79192 to 5.816968 eV that confirms that selected phytochemicals has stable structure and the band gap energy value equivalent to the band gap energy value of the bioactive molecules (Tamer et al.

Table 5 Predicted toxicity values of selected bioactive phytochemicals

Model name	Asperuloside	Asperulosidic acid	Deacetylasperulosidic acid	Eugenol	Rutin
AMES toxicity	No	No	No	Yes	No
Max. tolerated dose (human)	0.027	0.592	1.054	1.024	0.452
hERG I inhibitor	No	No	No	No	No
hERG II inhibitor	No	No	No	No	Yes
Oral rat acute toxicity (LD50)	2.262	2.344	2.154	2.118	2.491
Oral rat chronic toxicity (LOAEL)	3.426	3.641	3.362	2.049	3.673
Hepatotoxicity	No	No	No	No	No
Skin sensitization	No	No	No	Yes	No
T. Pyriformis toxicity	0.285	0.285	0.285	0.3	0.285
Minnow toxicity (log mM)	6.763	8.4	8.012	1.702	7.677

2012).The lower value of electron affinity represents the greater molecular reactivity with nucleophiles and among the five compound eugenol showed the lowest electron affinity whereas asperulosidic acid exhibits higher electron affinity. The higher hardness and lower softness values confirm the higher molecular hardness allied with the molecules. The chemical potential of the selected phytochemicals were negative which means the molecules were stable and it is one of the important properties for the bioactive molecules. The lower chemical potential and higher electrophilicity index values identified for phytochemicals and nucleophilicity index and electrophilicity index are also related to the biological activity of a molecule. The reactivity of a molecule increasing with increased nucleophilicity index (Azad et al. 2020). Here, among the five phytochemicals eugenol has higher nucleophilicity with 0.6437757 eV. Understanding the biological activity of certain phytochemicals can help predict their involvement in the human body. Monitoring absorption, distribution, metabolism, and excretion, which are all ADME features, is used to predict bioactivity (Yadav et al. 2020). This is crucial in evaluating the phytochemical's efficacy against the chosen target, MAPK6. The absorption process is the first step in transferring the phytochemicals that have been delivered. In this scenario, eugenol has been discovered to have higher water solubility, making it easier to absorb through the gastrointestinal tract (GI tract). The value we have facilitates us to estimate the efficacy of phytochemical absorption through the GI tract. When medicine is absorbed, it must have to go through a distribution process that describes the compound's whole bioactivity, which involves the permeability of the molecule. In general, the molecules offered for distribution do not reach the target in their entirety; instead, they dissolve and only a small percentage of them reach the target. As a result, the compound's bioactivity appears to be reduced. When compared to all other phytochemicals, eugenol has a high permeability. Its capacity to cross the blood–brain barrier and the CNS aids in its distribution throughout a broad span of the human body. Although these numbers provide a good starting point for anticipating bioactivity, more study, including clinical trials, is needed to acquire a clear picture of the process. In addition, in vivo excretion analysis aids us in characterizing the drug-likeness properties more eloquently. With a total clearance of 1.351, it appears that the drug's total clearance is perfectly sufficient, and the renal organic transporter (OCT2) has no effect on the phytochemicals utilized. While understanding bioactivity is important, understanding side effects and toxicity qualities is crucial when it comes to authorizing a medication. There is a widespread perception that herbal treatments are invariably associated with more severe adverse effects. Herbal medicines, on the other hand, are significantly more effective and have lower toxicity than synthetic drugs (Rathore et al. 2012). According to our findings, the phytochemicals examined exhibit no hepatotoxicity, except for eugenol in the case of no skin sensitivity. Except for one phytochemical, the AMES values appear to be satisfactory, and the LD50 values appear to be adequate when compared to the other data. Except for rutin, hERG II appears to have no inhibitors in phytochemicals. Thus, by knowing the toxicological property of *M. citrifolia* fruit, we may use it to interface with the human body in a wide number of alternative ways for the treatment of cancer.

Conclusion

The results from this current investigation revealed that all the bioactive phytochemicals from the *M. citrifolia* fruit exhibited good binding affinity at the active sites of MAPK6 protein, suggesting them as potential compounds that could inhibit cancer in human. Binding of these bioactive phytochemicals to target protein MAPK6 could inhibit or regulate cell metabolism, proliferation and apoptosis. Among 23 phytochemicals, five of the phytochemicals (asperuloside, asperulosidic acid, deacetylasperulosidic acid, eugenol and rutin) showed higher binding affinity (> -6.5 kcal/mol) against MAPK6 and compound rutin showed the highest docking score of -7.9 kcal/mol. Then the RC plot analysis showed the stable linkage based on structure and rotation for the protein–ligand interaction. The molecular reactivity, kinetic stability, and intramolecular charge transfer of the molecule are all factors that influence the bioactivity of the selected five phytochemicals, according to FMOs research and the stability and reactivity were evaluated through band gap energy values. These five compounds were further evaluated ADMET properties and those results showed that these five phytochemicals would be good drug candidates and relatively low or no toxic effects in human. However, further in vivo and in vitro studies are needed to further explore their activities and efficacies against human cancer.

Supplementary Information The online version contains supplementary material available at https://doi.org/10.1007/s40203-022-00130-4.

Author contributions The work was carried out in collaboration among all authors. The retrieval of bioactive phytochemicals and active site prediction was performed by DIS and AZ. The molecular docking and drug-likeness investigation was performed by KC and analyzed by AZ. The RC plot analysis was performed and validated by DIS and TK. Density function Theory was performed and analyzed by ABS and AZ. Validation of the manuscript was done by AZ. The whole write up of the manuscript was done in collaboration of all authors. All authors read and approved the final manuscript.

Funding The authors declare that no funds, grants, or other support were received during this study.

Declarations

Conflict of interest The authors have no relevant financial or non-financial interests to disclose.

Ethics approval Not applicable.

Consent to participate Not applicable.

Consent for publication Not applicable.

References

Ahmed B, Ashfaq UA, ul Qamar MT, Ahmad M (2014) Anti-cancer potential of phytochemicals against breast cancer: molecular docking and simulation approach. Bangladesh J Pharmacol 9(4):545–550

Al-Omary FA, Mary YS, Panicker CY, El-Emam AA, Al-Swaidan IA, Al-Saadi AA, Van Alsenoy C (2015) Spectroscopic investigations, NBO, HOMO–LUMO, NLO analysis and molecular docking of 5-(adamantan-1-yl)-3-anilinomethyl-2, 3-dihydro-1, 3, 4-oxadiazole-2-thione, a potential bioactive agent. J Mol Struct 1096:1–14. https://doi.org/10.1016/j.molstruc.2015.03.049

Alsaran HM (2016) Functional characterization of cancer-related mutations of ERK3

Azad I, Akhter Y, Khan T, Azad MI, Chandra S, Singh P et al (2020) Synthesis, quantum chemical study, AIM simulation, in silico ADMET profile analysis, molecular docking and antioxidant activity assessment of aminofuran derivatives. J Mol Struct 1203:127285. https://doi.org/10.1016/j.molstruc.2019.127285

Berman HM, Westbrook J, Feng Z, Gilliland G, Bhat TN, Weissig H et al (2000) The protein data bank. Nucleic Acids Res 28(1):235–242. https://doi.org/10.1093/nar/28.1.235

Bessong PO, Rojas LB, Obi LC, Tshisikawe PM, Igunbor EO (2006) Further screening of Venda medicinal plants for activity against HIV type 1 reverse transcriptase and integrase. Afr J Biotech 5(6):526–528

Bogucka K, Pompaiah M, Marini F, Binder H, Harms G, Kaulich M et al (2020) ERK3/MAPK6 controls IL-8 production and chemotaxis. Elife. https://doi.org/10.7554/eLife.52511

Calzuola I, Luigi Gianfranceschi G, Marsili V (2006) Comparative activity of antioxidants from wheat sprouts, *Morinda citrifolia*, fermented papaya and white tea. Int J Food Sci Nutr 57(3–4):168–177. https://doi.org/10.1080/09637480600658328

Cargnello M, Roux PP (2011) Activation and function of the MAPKs and their substrates, the MAPK-activated protein kinases. Microbiol Mol Biol Rev 75(1):50–83. https://doi.org/10.1128/MMBR.00031-10

Chan-Blanco Y, Vaillant F, Perez AM, Reynes M, Brillouet JM, Brat P (2006) The noni fruit (*Morinda citrifolia* L.): a review of agricultural research, nutritional and therapeutic properties. J Food Compos Anal 19(6–7):645–654. https://doi.org/10.1016/j.jfca.2005.10.001

Conlon JM, Sonnevend A, Patel M, Davidson C, Nielsen PF, Pal T, Rollins-Smith LA (2003) Isolation of peptides of the brevinin-1 family with potent candidacidal activity from the skin secretions of the frog *Rana boylii*. J Pept Res 62(5):207–213. https://doi.org/10.1034/j.1399-3011.2003.00090.x

Dallakyan S, Olson AJ (2015) Small-molecule library screening by docking with PyRx. In: Chemical biology. Humana Press, New York, NY, pp 243–250

Erratum: Global Cancer Statistics 2018 (2020) GLOBOCAN estimates of incidence and mortality worldwide for 36 cancers in 185 countries. CA Cancer J Clin 70(4):313

Ganesan V, Gurumani V, Kunjiappan S, Panneerselvam T, Somasundaram B, Kannan S et al (2018) Optimization and analysis of microwave-assisted extraction of bioactive compounds from *Mimosa pudica* L. using RSM & ANFIS modeling. J Food Meas Charact 12(1):228–242. https://doi.org/10.1007/s11694-017-9634-y

Ghasemzadeh A, Jaafar HZ, Rahmat A (2010) Antioxidant activities, total phenolics and flavonoids content in two varieties of Malaysia young ginger (*Zingiber officinale* Roscoe). Molecules 15(6):4324–4333. https://doi.org/10.3390/molecules15064324

Jasril LN, Mooi LY, Abdullah MA, Sukari MA, Ali AM (2003) Anti-tumor promoting and antioxidant activities of anthraquinones isolated from the cell suspension culture of *Morinda elliptica*. Asia Pac J Mol Biol Biotechnol 11(1):3–7

Kushi LH, Doyle C, McCullough M, Rock CL, Demark-Wahnefried W, Bandera EV, American Cancer Society 2010 Nutrition and Physical Activity Guidelines Advisory Committee et al (2012) American Cancer Society guidelines on nutrition and physical activity for cancer prevention: reducing the risk of cancer with healthy food choices and physical activity. CA Cancer J Clin 62(1):30–67. https://doi.org/10.3322/caac.20140

Long W, Foulds CE, Qin J, Liu J, Ding C, Lonard DM et al (2012) ERK3 signals through SRC-3 coactivator to promote human lung cancer cell invasion. J Clin Investig 122(5):1869–1880. https://doi.org/10.1172/JCI61492

Mallath MK, Taylor DG, Badwe RA, Rath GK, Shanta V, Pramesh CS et al (2014) The growing burden of cancer in India: epidemiology and social context. Lancet Oncol 15(6):e205–e212. https://doi.org/10.1016/S1470-2045(14)70115-9

Mates JM (2000) Effects of antioxidant enzymes in the molecular control of reactive oxygen species toxicology. Toxicology 153(1–3):83–104. https://doi.org/10.1016/S0300-483X(00)00306-1

McClatchey W (2002) From Polynesian healers to health food stores: changing perspectives of *Morinda citrifolia* (Rubiaceae). Integr Cancer Ther 1(2):110–120. https://doi.org/10.1177/1534735402001002002

Mohanraj K, Karthikeyan BS, Vivek-Ananth RP, Chand RP, Aparna SR, Mangalapandi P, Samal A (2018) IMPPAT: a curated database of Indian medicinal plants, phytochemistry and therapeutics. Sci Rep 8(1):1–17. https://doi.org/10.1038/s41598-018-22631-z

Nordberg J, Arnér ES (2001) Reactive oxygen species, antioxidants, and the mammalian thioredoxin system. Free Radical Biol Med 31(11):1287–1312. https://doi.org/10.1016/S0891-5849(01)00724-9

Novena LM, Athimoolam S, Anitha R, Bahadur SA (2022) Synthesis, crystal structure, hirshfeld surface analysis, spectral and quantum chemical studies of pharmaceutical cocrystals of a bronchodilator drug (Theophylline). J Mol Struct 1249:131585. https://doi.org/10.1016/j.molstruc.2021.131585

Palmeira CM, Teodoro JS, Amorim JA, Steegborn C, Sinclair DA, Rolo AP (2019) Mitohormesis and metabolic health: the interplay between ROS, cAMP and sirtuins. Free Radical Biol Med 141:483–491. https://doi.org/10.1016/j.freeradbiomed.2019.07.017

Pawlus AD, Su BN, Keller WJ, Kinghorn AD (2005) An anthraquinone with potent quinone reductase-inducing activity and other constituents of the fruits of *Morinda citrifolia* (Noni). J Nat Prod 68(12):1720–1722. https://doi.org/10.1021/np050383k

Perše M (2014) The role of the antioxidant defense system in the pathogenesis of colorectal cancer. Free Radic 217

Phakhodee W (2012) Distribution of naturally occurring anthraquinones, iridoids and flavonoids from Morinda genus: chemistry and biological activity. Walailak J Sci Technol (WJST) 9(3):173–188

Potterat O, Hamburger M (2007) *Morinda citrifolia* (Noni) fruit-phytochemistry, pharmacology, safety. Planta Med 73(03):191–199

Prashanth J, Ramesh G, Naik JL, Ojha JK, Reddy BV (2016) Molecular geometry, NBO analysis, hyperpolarizability and HOMO-LUMO energies of 2-azido-1-phenylethanone using quantum chemical calculations. Mater Today Proc 3(10):3761–3769. https://doi.org/10.1016/j.matpr.2016.11.025

Rathore SK, Bhatt SHASHANK, Dhyani S, Jain A (2012) Preliminary phytochemical screening of medicinal plant *Ziziphus mauritiana* Lam. fruits. Int J Curr Pharm Res 4(3):160–162

Ren J, Sowers JR, Zhang Y (2018) Autophagy and cardiometabolic diseases: from molecular mechanisms to translational medicine. Academic Press, Cambridge

Roux PP, Blenis J (2004) ERK and p38 MAPK-activated protein kinases: a family of protein kinases with diverse biological functions. Microbiol Mol Biol Rev 68(2):320–344. https://doi.org/10.1128/MMBR.68.2.320-344.2004

Ruksilp T, Sichaem J, Khumkratok S, Siripong P, Tip-pyang S (2011) Anthraquinones and an iridoid glycoside from the roots of *Morinda pandurifolia*. Biochem Syst Ecol 39(4–6):888–892

Sachdev S, Ansari SA, Ansari MI, Fujita M, Hasanuzzaman M (2021) Abiotic stress and reactive oxygen species: generation, signaling, and defense mechanisms. Antioxidants 10(2):277. https://doi.org/10.3390/antiox10020277

Salhi S, Fadli M, Zidane L, Douira A (2010) Etudes floristique et ethnobotanique des plantes médicinales de la ville de Kénitra (Maroc). Mediterr Bot 31:133

Tamer Ö, Sarıboğa B, Ucar I (2012) A combined crystallographic, spectroscopic, antimicrobial, and computational study of novel dipicolinate copper(II) complex with 2-(2-hydroxyethyl) pyridine. Struct Chem 23(3):659–670. https://doi.org/10.1007/s11224-011-9910-0

Viswanathan TM, Chitradevi K, Zochedh A, Vijayabhaskar R, Sukumaran S, Kunjiappan S et al (2022) Guanidine–curcumin complex-loaded amine-functionalised hollow mesoporous silica nanoparticles for breast cancer therapy. Cancers 14(14):3490. https://doi.org/10.3390/cancers14143490

Walton NJ, Brown DE (1999) Chemicals from plants: perspectives on plant secondary products. World Scientific, Singapore

Wang MY, West BJ, Jensen CJ, Nowicki D, Su C, Palu AK, Anderson G (2002) *Morinda citrifolia* (Noni): a literature review and recent advances in Noni research. Acta Pharmacol Sin 23(12):1127–1141

Wang Y, Liu H, Fan Y, Chen X, Yang Y, Zhu L et al (2019) In silico prediction of human intravenous pharmacokinetic parameters with improved accuracy. J Chem Inf Model 59(9):3968–3980. https://doi.org/10.1021/acs.jcim.9b00300

Whistler WA (1985) Traditional and herbal medicine in the Cook Islands. J Ethnopharmacol 13(3):239–280. https://doi.org/10.1016/0378-8741(85)90072-8

Wisniewski D, Lambek CL, Liu C, Strife A, Veach DR, Nagar B et al (2002) Characterization of potent inhibitors of the Bcr-Abl and the c-kit receptor tyrosine kinases. Can Res 62(15):4244–4255

Xiao H, Lü F, Stewart D, Zhang Y (2013) Mechanisms underlying chemopreventive effects of flavonoids via multiple signaling nodes within Nrf2-ARE and AhR-XRE gene regulatory networks. Curr Chem Biol 7(2):151–176

Yadav A, Honamane P, Rajput M, Dange V, Salunkhe K, Kane S, Mohite S (2020) Antimalarial activity of *Psidium guajava* leaf extracts. Int J Sci Res Chemi 5(6):63–68

Zhuo LG, Liao W, Yu ZX (2012) A frontier molecular orbital theory approach to understanding the Mayr equation and to quantifying nucleophilicity and electrophilicity by using HOMO and LUMO energies. Asian J Org Chem 1(4):336–345. https://doi.org/10.1002/ajoc.201200103

Zochedh A, Priya M, Shunmuganarayanan A, Thandavarayan K, Sultan AB (2022) Investigation on structural, spectroscopic, DFT, biological activity and molecular docking simulation of essential oil Gamma-Terpinene. J Mol Struct. https://doi.org/10.1016/j.molstruc.2022.133651